Modeling of stresses and electric fields in piezoelectric multilayer: Application to multi quantum wells

Dhaneshwar Mishra, Soong Hyeong Lee, Youjung Seo, and Y. Eugene Pak

Citation: AIP Advances **7**, 075306 (2017); doi: 10.1063/1.4991836
View online: http://dx.doi.org/10.1063/1.4991836
View Table of Contents: http://aip.scitation.org/toc/adv/7/7
Published by the American Institute of Physics

Modeling of stresses and electric fields in piezoelectric multilayer: Application to multi quantum wells

Dhaneshwar Mishra,[1] Soong Hyeong Lee,[2] Youjung Seo,[1]
and Y. Eugene Pak[1,a]
[1]*Advanced Institutes of Convergence Technology, Seoul National University, Suwon 443-270, South Korea*
[2]*Department of Physics, Ajou University, Suwon 443-749, South Korea*

(Received 24 March 2017; accepted 22 June 2017; published online 12 July 2017)

Exact closed-form expressions have been derived for the stresses and the electric fields induced in piezoelectric multilayers deposited on a substrate with lattice misfit and thermal expansion coefficient mismatch. The derived formulations can model any number of layers using recursive relations that minimize the computation time. A proper rotation matrix has been utilized to generalize the expressions so that they can be used for various growth orientations with each layer having hexagonal crystal symmetry. As an example, the influence of lattice misfit and thermal expansion coefficient mismatch on the state of electroelastic fields in different layers of GaN multi quantum wells has been examined. A comparison with the finite element analysis results showed very close agreement. The analytical expressions developed herein will be useful in designing optoelectronic devices as well as in predicting defect density in multi quantum wells. [http://dx.doi.org/10.1063/1.4991836]

I. INTRODUCTION

Piezoelectric multilayers are widely used in high performance sensors, actuators and electronic devices. LEDs and other optoelectronic devices are fabricated mostly by nitride-based materials that have hexagonal crystal symmetry. The multi quantum wells in these devices can be fabricated in different growth orientations such as *c*-plane, *a*-plane, *m*-plane, and semi-polar planes. Each layer of these devices can have different lattice parameters and thermal expansion coefficients that give rise to misfit and thermal strains. Furthermore, the piezoelectric properties of these layers lead to electric field generation in each layer. Since the strains and electric fields in the layers can influence the optoelectronic device performance, the quantification of their magnitudes is of importance. They can also be important in predicting the formations of defects and their densities. Therefore, it would be very useful to have analytical expressions that can readily provide the stress and electric field distributions in each layer, given the lattice and thermal expansion coefficients mismatches. The analytical prediction tool developed herein can be very useful in optoelectronic device design particularly when piezoelectrically generated electric field needs to be taken into account.

There are many works available in the literature on modeling of elastic multilayers deposited on a thick substrate. Most of them are based on the beam bending theory first developed by Stoney in 1909.[1] There are many modifications of the original model to accommodate for variety of applications. Townsend and Barnett developed the elastic relationships in layered composite media and devised the approximation formula for the case of thin films on a thick substrate.[2] The multilayer models available in the literature are shown to be computationally cumbersome as they require solving simultaneous equations in obtaining the solution. This feature increases the computation time

[a]Electronic mail: genepak@snu.ac.kr

with the number of layers modeled. It will be even more difficult if anisotropic layers are considered giving rise to anisotropic strain and stress fields. In this regard, Freund developed a two parameter model for the stress distribution by defining a reference plane, a reference strain and a reference curvature for compositionally graded thin films.[3,4] Some multilayer models were developed based on the Freund's model defining the reference plane arbitrarily.[5,6] These models require solving the simultaneous equations which can turn out to be complicated even for two parameter models. There are some other works available in the literature on multilayer thin films deposited on a substrate which are subjected to non-uniform misfit strains and non-uniform temperatures derived by modifying the original Stoney formula to evaluate stresses and curvature in each layer.[7,8] Hsueh et al. provided analytical formulations for thermal stresses in joining two layers with multi and graded interlayers.[9] Recently, Gao et al. developed an elastic multilayer model in evaluating the thermal stress distribution in a multilayer coating by defining the reference plane at the neutral axis when the multilayer system is subjected to bending only.[10] This model avoids solving simultaneous equations as it calculates the total curvature and the inplane reference strains in place of calculating these parameters for individual layer. This can greatly reduce the computation time and complications in the calculations.

There are number of works available on modeling piezoelectric multilayers applicable to sensors and actuators.[11–20] Nehjad et al. modeled intrinsic strain in the layered piezoelectric structure and evaluated residual stresses in each layer of the piezoelectric microelectromechanical systems.[21] There are also many works available on evaluating the stress fields in multilayered nitride-based devices considering them as purely elastic media.[22,23] There were attempts made to calculate the electric fields and optical transitions in InGaN/GaN quantum wells by developing a piezoelectric multilayer theory that holds the total electric displacement in the multilayer to be constant while the total electric field is made to vanish.[24] However, there is very little work are available in the literature on the analytical models applicable to piezoelectric multilayers especially for modeling optoelectronic multi quantum wells. To the best of authors' knowledge, there is no analytical model available providing the closed-form expressions that can handle piezoelectricity in each layer having various crystal orientations of hexagonal class.

To this end, a closed-form solution for the electroelastic fields has been derived that predicts the curvatures and the normal strains in the piezoelectric multilayer. As an example, specific results for inplane stresses and electric fields have been calculated for a GaN-based multi quantum well device with 12 thin film layers deposited in various growth orientations, namely *c*-, *a*- and *m*-planes, on a thick sapphire substrate. These results are validated by modeling the multi quantum well layers using the commercial finite element analysis code ABAQUS 6.14. The influence of thermal expansion coefficient and lattice mismatches on the electroelastic fields are examined along with the effects of piezoelectricity in different growth orientations.

II. ANALYSIS AND RESULTS

This work is the generalization of the elastic multilayer formulation given by Gao et al.,[10] hence, the same general methodologies have been followed. In particular, this work includes transversely isotropic material properties belonging to a hexagonal crystal class exhibiting piezoelectricity and spontaneous polarization. This work also introduces the rotation matrix so that one can obtain the closed-form expressions for various growth orientations. In addition to the thermal strain, our formulation also includes strains arising from lattice misfit between the film layers. This model also accounts for different inplane strains and curvatures along the mutually orthogonal directions arising from anisotropic material properties. These additional considerations in the analytical model makes the solution somewhat more complicated, however, the main approach here is simple in that the lattice misfit and thermal mismatch in each layer give rise to extensional or compressive strains that collectively induces bending in the multilayer. The intrinsic piezoelectricity and spontaneous polarization along [0001] crystal direction in different layers give rise to electric fields. It is assumed that only normal strains are induced in the multilayer, which give rise to only normal stresses. Therefore, the shear stresses and strains are considered to be zero everywhere. We solve the problem by dividing it into three components, namely, the reference inplane normal strains arising from

the extension/compression of the multilayer (ε^N_{xx}, ε^N_{yy}), the reference curvature components due to bending (K_x, K_y), and the strains due to layer-wise lattice misfit ($\varepsilon^{m^i}_{ij}$), and strains due to thermal mismatch ($\varepsilon^{T^i}_{ij}$). The sum of $\varepsilon^{m^i}_{ij}$ and $\varepsilon^{T^i}_{ij}$ is being treated as the total mismatch strain, $\varepsilon^{M^i}_{ij}$. The inplane normal strains due to lattice misfit between the consecutive layers are considered to be constant for each layer. We solve these problems separately using the linear piezoelectric constitutive relations and then invoke superposition principle to evaluate the layer-wise stresses and electric fields.

A. Piezoelectric multilayer formulation

A piezoelectric multilayer is schematically shown in Fig. 1, where n layers of the piezoelectric films with individual thickness, t_i (i = 1, 2,.., n), are bonded sequentially to a substrate with thickness t_0. The first layer of the piezoelectric multilayer is in direct contact with the substrate. The coordinate system is defined such that the substrate bottom surface is located at z = 0, the free surface of the multilayer is located at $z = h_{n+1}$, and the interface between layers i and i+1 is located at $z = h_{i+1}$. The relation between h_i and t_i can be expressed as[10]

$$h_i = \sum_{j=0}^{i-1} t_j \qquad \text{(i = 1 to n + 1).} \tag{1}$$

The multilayer is deposited on a substrate with different lattice parameters and different coefficients of thermal expansion. During the fabrication process, these layers are deposited at an elevated temperature and subsequently cooled down. Hence, the lattice mismatch and the coefficients of thermal expansion mismatch between the consecutive film layers collectively induce the overall

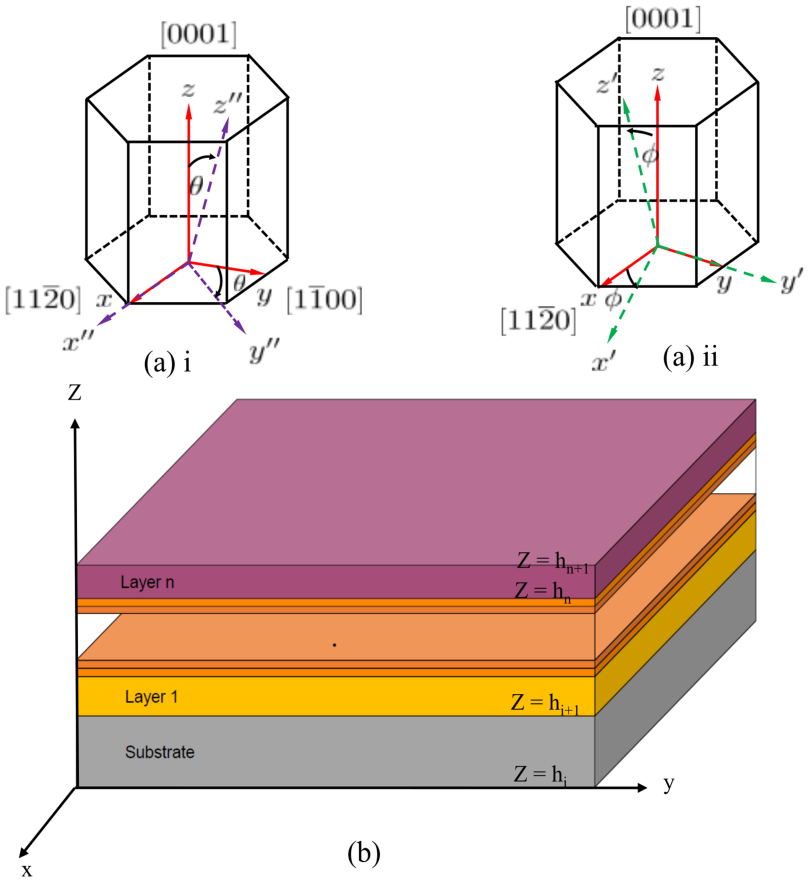

FIG. 1. Schematic representation of n layers multilayer and growth orientations.

extensional or compressive strain as well as the bending of the whole multilayer. Each layers are piezoelectric, therefore, the strains can produce electric fields in each layer.

The total strain in the multilayer system consists of the reference inplane strains (ε^N_{xx}, ε^N_{yy}) and the bending strains (ε^B_{xx}, ε^B_{yy}) such that

$$\varepsilon^{Tot}_{xx} = \varepsilon^N_{xx} + \varepsilon^B_{xx} \qquad \textit{and} \qquad \varepsilon^{Tot}_{yy} = \varepsilon^N_{yy} + \varepsilon^B_{yy}, \tag{2}$$

where $\varepsilon^B_{xx} = K_x(z - \Pi_x)$ and $\varepsilon^B_{yy} = K_y(z - \Pi_y)$ with $z = \Pi_x$, $z = \Pi_y$ defining the location of the reference plane on which the bending strain is zero. The x- and y-components of both the strains and the curvatures are considered to be different due to material anisotropy. The electric field components due to the reference normal and bending strains can be expressed as

$$E^{Tot^i}_k = E^{N^i}_k + E^{B^i}_k, \tag{3}$$

where k denotes the coordinates x, y and z. As discussed above, the inplane and the out-of-plane shear components of both the strains and stresses are zero for the considered piezoelectric multilayer ($\varepsilon_{zx} = \varepsilon_{zy} = \varepsilon_{xy} = \sigma_{zx} = \sigma_{zy} = \sigma_{xy} = 0$). This assumption leads to the vanishing of electric fields and electric displacements along the x- and y-axes ($E^{Tot}_x = E^{Tot}_y = D^{Tot}_x = D^{Tot}_y = 0$) when the constitutive relations shown in Appendix A are used.

The constitutive relations for hexagonal crystals (Appendix A) are given such that the c-axis [0001] of the crystal is aligned with the z-direction (Fig. 1), while the crystal directions $[11\bar{2}0]$ and $[1\bar{1}00]$ are aligned with the x- and y-axes, respectively. We would like to consider two sets of rotations, namely about $[11\bar{2}0]$ direction where $[1\bar{1}00]$ and [0001] rotate by an angle ϕ, while the rotation about $[1\bar{1}00]$ rotates the other two crystal directions by an angle θ. The combined rotation matrix can be expressed as

$$[U] = \begin{bmatrix} \cos\theta & 0 & -\sin\theta \\ \sin\theta\sin\phi & \cos\phi & \cos\theta\sin\phi \\ \sin\theta\cos\phi & -\sin\phi & \cos\theta\cos\phi \end{bmatrix}.$$

The solution has been derived for the electroelastic fields in the piezoelectric multilayer for three popular growth orientations, namely, c-plane ($\phi = \theta = 0$), a-plane ($\phi = \pi/2$, $\theta = 0$) and m-plane ($\phi = 0$, $\theta = \pi/2$). Here, the crystal directions are rotated in accordance with the growth direction, while x-, y- and z-axes are fixed to the global geometry of the multilayer, i.e., the x- and y-axes are always the inplane directions while the z-axis is the growth direction. Therefore, for the c-plane growth, the z-axis is aligned with [0001] direction while x- and y-axes are associated with $[11\bar{2}0]$ and $[1\bar{1}00]$ directions, respectively. These assignments change for the a- and m-plane growth, where the crystal growth direction $[11\bar{2}0]$ is aligned with the z-axis for the a-plane growth, and the crystal direction $[1\bar{1}00]$ is aligned with the z-axis for the m-plane growth.

The stresses and the electric displacements in the i^{th} layer of the multilayer with [0001] crystal axis as the growth direction can be expressed using the constitutive relations provided in Appendix A. After discarding the shear stresses which are assumed to be zero in this work along with the inplane electric displacement components turn out to be zero based on the assumptions made and properly utilizing the rotation matrix above, the state of normal stresses and electric displacement along [0001] crystal direction for a generalized orientation can be expressed as

$$\begin{Bmatrix} \sigma^i_{xx} \\ \sigma^i_{yy} \\ \sigma^i_{zz} \\ D^i_{[0001]} \end{Bmatrix} = \begin{bmatrix} A^i_{11} & A^i_{12} & A^i_{13} & -e^i_1 \\ A^i_{21} & A^i_{22} & A^i_{23} & -e^i_2 \\ A^i_{31} & A^i_{32} & A^i_{33} & -e^i_3 \\ e^i_1 & e^i_2 & e^i_3 & \epsilon^i_{33} \end{bmatrix} \begin{Bmatrix} \varepsilon^N_{xx} + \varepsilon^B_{xx} - \varepsilon^{m^i}_{xx} - \varepsilon^{T^i}_{xx} \\ \varepsilon^N_{yy} + \varepsilon^B_{yy} - \varepsilon^{m^i}_{yy} - \varepsilon^{T^i}_{yy} \\ \varepsilon^{N^i}_{zz} + \varepsilon^{B^i}_{zz} - \varepsilon^{m^i}_{zz} - \varepsilon^{T^i}_{zz} \\ E^{N^i}_{[0001]} + E^{B^i}_{[0001]} - E^{M^i}_{[0001]} \end{Bmatrix} + \begin{Bmatrix} 0 \\ 0 \\ 0 \\ P^i_{sp} \end{Bmatrix}, \tag{4}$$

where $i = 0$ stands for the substrate while $i = 1, \ldots, n$ stands for different layers of the piezoelectric multilayer film. The A_{ij} and e_i are rotated anisotropic elastic and piezoelectric material constants, respectively, which can be expressed as

$$[A] = [U] \begin{bmatrix} c_{11} & c_{12} & c_{13} \\ c_{12} & c_{11} & c_{13} \\ c_{13} & c_{13} & c_{33} \end{bmatrix} [U]^T \qquad \begin{Bmatrix} e_1 \\ e_2 \\ e_3 \end{Bmatrix} = [U] \begin{Bmatrix} e_{31} \\ e_{31} \\ e_{33} \end{Bmatrix},$$

while ϵ_{33} is the materials's dielectric constant. Here, $\varepsilon_{xx}^{m^i}$ and $\varepsilon_{yy}^{m^i}$ are the inplane strains arising from the lattice mismatch between the consecutive layers, where as $\varepsilon_{zz}^{N^i}$, $\varepsilon_{zz}^{B^i}$, $\varepsilon_{zz}^{m^i}$ are, respectively, the out-of-plane normal reference strain, bending strain, and the strain due to lattice misfit. The thermal strains, $\varepsilon_{ij}^{T^i}$, can be expressed as

$$\begin{Bmatrix} \varepsilon_{xx}^T \\ \varepsilon_{yy}^T \\ \varepsilon_{zz}^T \end{Bmatrix} = [U] \begin{bmatrix} \alpha_a & 0 & 0 \\ 0 & \alpha_a & 0 \\ 0 & 0 & \alpha_c \end{bmatrix} [U]^T \Delta T,$$

where α_a is the thermal expansion coefficient along $[11\bar{2}0]$ and $[1\bar{1}00]$ directions and α_c is the thermal expansion coefficients along [0001] direction. $E_{[0001]}^{M^i}$ is the electric field component due to lattice and thermal mismatches and P_{sp}^i is the spontaneous polarization along [0001] direction.

The out-of-plane normal stress, σ_{zz}, and electric displacement, $D_{[0001]}$, are considered to be matched at each interface, i.e., $\sigma_{zz}^i = \sigma_{zz}^{i+1}$ and $D_{[0001]}^i = D_{[0001]}^{i+1}$. At the free surfaces and edges, the traction free and charge free boundary conditions are applied, i.e., $\sigma_{zz}^{(i=0)} = D_{[0001]}^{(i=0)} = 0$. These conditions are utilized to evaluate the out-of-plane normal strain, ε_{zz}^i, and the electric field, $E_{[0001]}^i$ in each layer.

B. Normal stresses in multilayer

1. Inplane stresses due to reference and mismatch strains

The inplane reference strain components, ε_{xx}^N and ε_{yy}^N, and the mismatch strains arising from lattice mismatch, ε_{xx}^m and ε_{yy}^m, and the thermal mismatch, ε_{ij}^T, respectively, are constant in each layer, i.e., does not vary through the thickness. The interlayer continuity conditions and the boundary condition at the bottom surface of the substrate give rise to $\sigma_{zz}^{i=0} = \sigma_{zz}^{i=1}$ and $D_{[0001]}^{i=0} = D_{[0001]}^{i=1}$. Therefore, it turns out that $\sigma_{zz}^i = D_{[0001]}^i = 0$, where $i = 0, 1, 2, \ldots$.n. These conditions were used to evaluate the out-of-plane normal strain components, $\varepsilon_{zz}^{N^i}$ and $\varepsilon_{zz}^{m^i}$, and the electric fields, $E_{[0001]}^{N^i}$ and $E_{[0001]}^{M^i}$. The inplane stresses arising from the reference inplane strains, ε_{xx}^N and ε_{yy}^N can be expressed as

$$\begin{aligned} \sigma_{xx}^{N^i} &= Q_1^i \varepsilon_{xx}^N + Q_2^i \varepsilon_{yy}^N \\ \sigma_{yy}^{N^i} &= Q_3^i \varepsilon_{xx}^N + Q_4^i \varepsilon_{yy}^N, \end{aligned} \tag{5}$$

and the inplane stresses due to lattice and thermal mismatch can be expressed as

$$\begin{aligned} \sigma_{xx}^{M^i} &= Q_1^i (\varepsilon_{xx}^{m^i} + \varepsilon_{xx}^{T^i}) + Q_2^i (\varepsilon_{yy}^{m^i} + \varepsilon_{yy}^{T^i}) - \frac{e_1^i P_{sp}^i}{A_3^i} \\ \sigma_{yy}^{M^i} &= Q_3^i (\varepsilon_{xx} m^i + \varepsilon_{xx}^{T^i}) + Q_4^i (\varepsilon_{yy}^{m^i} + \varepsilon_{yy}^{T^i}) - \frac{e_2^i P_{sp}^i}{A_3^i}, \end{aligned} \tag{6}$$

where

$$\begin{aligned} Q_1^i &= A_{11}^i - \frac{A_{13}^i A_1^i}{A_3^i} - \frac{e_1^i}{e_3^i}\left(A_{31}^i - \frac{A_{33}^i A_1^i}{A_3^i}\right) \\ Q_2^i &= A_{12}^i - \frac{A_{13}^i A_2^i}{A_3^i} - \frac{e_2^i}{e_3^i}\left(A_{32}^i - \frac{A_{33}^i A_2^i}{A_3^i}\right) \\ Q_3^i &= A_{21}^i - \frac{A_{23}^i A_1^i}{A_3^i} - \frac{e_2^i}{e_3^i}\left(A_{31}^i - \frac{A_{33}^i A_1^i}{A_3^i}\right) \\ Q_4^i &= A_{22}^i - \frac{A_{23}^i A_2^i}{A_3^i} - \frac{e_2^i}{e_3^i}\left(A_{32}^i - \frac{A_{33}^i A_2^i}{A_3^i}\right) \end{aligned}$$

and

$$A_1 = (e_3 e_1 + A_{31}\epsilon_{33}) \qquad A_2 = (e_3 e_2 + A_{32}\epsilon_{33}) \qquad A_3 = \left(e_3^2 + A_{33}\epsilon_{33}\right).$$

2. Inplane stresses due to bending

The bending strains, $\varepsilon^{B}_{xx} = K_x(z - \Pi_x)$ and $\varepsilon^{B}_{yy} = K_y(z - \Pi_x)$, are functions of z, hence, linearly vary through the thickness. As discussed above, the out-of-plane normal stress, σ_{zz}, and electric displacement, $D_{[0001]}$, are continuous at the interfaces, i.e., $\sigma^{B^i}_{zz} = \sigma^{B^{i+1}}_{zz}$ and $D^{B^i}_{[0001]} = D^{B^{i+1}}_{[0001]}$. At the same time, they are zero at the bottom surface and at the free edges of the multilayer. These conditions have been used to calculate the out-of-plane normal strain, $\varepsilon^{B^i}_{zz}$, and the electric field, $E^{B^i}_{[0001]}$, in the substrate and in the film layers.

After the substitution of the out-of-plane normal strain, $\varepsilon^{B^0}_{zz}$, and the electric field, $E^{B^0}_{[0001]}$, the inplane bending stresses in the substrate can be expressed as

$$\begin{aligned}\sigma^{B^0}_{xx} &= A^0_{11}K_x z - Q^0_1 K_x \Pi_x + A^0_{12}K_y z - Q^0_2 K_y \Pi_y\\ \sigma^{B^0}_{yy} &= A^0_{21}K_x z - Q^0_3 K_x \Pi_x + A^0_{22}K_y z - Q^0_4 K_y \Pi_y.\end{aligned} \tag{7}$$

The inplane bending stresses in the $(i+1)^{th}$ layer of the multilayer can be expressed by substituting the out-of-plane normal strain, $\varepsilon^{B^{i+1}}_{zz}$, and the electric field along [0001], $E^{B^{i+1}}_{[0001]}$, into first two equations of Eq. (4)

$$\begin{aligned}\sigma^{B^{i+1}}_{xx} &= Q^{i+1}_5 K_x (z - \Pi_x) + Q^{i+1}_6 K_y \left(z - \Pi_y\right) + Q^{i+1}_7\\ \sigma^{B^{i+1}}_{yy} &= Q^{i+1}_8 K_x (z - \Pi_x) + Q^{i+1}_9 K_y \left(z - \Pi_y\right) + Q^{i+1}_{10},\end{aligned} \tag{8}$$

where

$$\begin{aligned}
Q^{i+1}_5 &= A^{i+1}_{11} + \frac{A^{i+1}_{13}B^{i+1}_2}{B^{i+1}_1} - \frac{e^{i+1}_1}{e^{i+1}_3}\left\{\left(A^i_{31} - A^{i+1}_{31}\right) - A^{i+1}_{33}\frac{B^{i+1}_2}{B^{i+1}_1}\right\}\\
Q^{i+1}_6 &= A^{i+1}_{12} + \frac{A^{i+1}_{13}B^{i+1}_3}{B^{i+1}_1} - \frac{e^{i+1}_1}{e^{i+1}_3}\left\{\left(A^i_{32} - A^{i+1}_{32}\right) - A^{i+1}_{33}\frac{B^{i+1}_3}{B^{i+1}_1}\right\}\\
Q^{i+1}_7 &= B^i_5 - \frac{A^{i+1}_{33}B^{i+1}_4}{B^{i+1}_1}\\
Q^{i+1}_8 &= A^{i+1}_{21} + \frac{A^{i+1}_{23}B^{i+1}_2}{B^{i+1}_1} - \frac{e^{i+1}_2}{e^{i+1}_3}\left\{\left(A^i_{31} - A^{i+1}_{31}\right) - A^{i+1}_{33}\frac{B^{i+1}_2}{B^{i+1}_1}\right\}\\
Q^{i+1}_9 &= A^{i+1}_{22} + \frac{A^{i+1}_{23}B^{i+1}_3}{B^{i+1}_1} - \frac{e^{i+1}_2}{e^{i+1}_3}\left\{\left(A^i_{32} - A^{i+1}_{32}\right) - A^{i+1}_{33}\frac{B^{i+1}_3}{B^{i+1}_1}\right\}\\
Q^{i+1}_{10} &= B^i_5 - \frac{A^{i+1}_{33}B^{i+1}_4}{B^{i+1}_1} \qquad\qquad B^{i+1}_1 = e^{(i+1)^2}_3 - \epsilon^{i+1}_{33}A^{i+1}_{33}\\
B^{i+1}_2 &= e^{i+1}_3(e^i_1 - e^{i+1}_1) - \epsilon^{i+1}_{33}(A^i_{31} - A^{i+1}_{31}) \qquad B^{i+1}_3 = e^{i+1}_3(e^i_2 - e^{i+1}_2) - \epsilon^{i+1}_{33}(A^i_{32} - A^{i+1}_{32})\\
B^{i+1}_4 &= (e^i_3 e^{i+1}_3 - \epsilon^{i+1}_{33}A^i_{33})\varepsilon^{B^i}_{zz} + \epsilon^{i+1}_{33}(e^{i+1}_3 - e^i_3)E^{B^i}_{[0001]}\\
B^i_5 &= A^i_{33}\varepsilon^{B^i}_{zz} - e^i_3 E^{B^i}_{[0001]}.
\end{aligned}$$

C. Position of neutral axes

The position of the neutral axes ($z = \Pi_x$, $z = \Pi_y$) can be calculated by equating the total inplane bending force components in the multilayer to be zero ($\sum_{i=0}^{n} F^{B^i}_x = \sum_{i=0}^{n} F^{B^i}_x = 0$). This results in

$$\begin{aligned}
\Pi_x &= \left[\frac{R_1}{R_2} - \frac{R_4(R_7 - R_1R_6/R_2)}{R_2(R_8 - R_4R_6/R_2)}\right] + \frac{K_x}{K_y}\left[\frac{R_3}{R_2} - \frac{R_4(R_9 - R_3R_6/R_2)}{R_2(R_8 - R_4R_6/R_2)}\right]\\
&\quad \frac{1}{K_x}\left[\frac{R_5}{R_2} - \frac{R_4(R_{10} - R_5R_6/R_2)}{R_2(R_8 - R_4R_6/R_2)}\right]\\
\Pi_y &= \left[\frac{(R_9 - R_3R_6/R_2)}{(R_8 - R_4R_6/R_2)} + \frac{K_x}{K_y}\frac{(R_7 - R_1R_6/R_2)}{(R_8 - R_4R_6/R_2)} + \frac{1}{K_x}\frac{R_{10} - (R_5R_6/R_2)}{(R_8 - R_4R_6/R_2)}\right],
\end{aligned} \tag{9}$$

where

$$R_1 = A_{11}^0 \frac{t_0^2}{2} + \sum_{i=0}^{n-1} Q_5^{i+1} \left(\frac{h_{i+2}^2}{2} - \frac{h_{i+1}^2}{2} \right) \qquad R_2 = Q_1^0 t_0 + \sum_{i=0}^{n-1} Q_5^{i+1} t_{i+1}$$

$$R_3 = A_{12}^0 \frac{t_0^2}{2} + \sum_{i=0}^{n-1} Q_6^{i+1} \left(\frac{h_{i+2}^2}{2} - \frac{h_{i+1}^2}{2} \right) \qquad R_4 = Q_2^0 t_0 + \sum_{i=0}^{n-1} Q_6^{i+1} t_{i+1}$$

$$R_5 = \sum_{i=0}^{n-1} Q_7^{i+1} t_{i+1} \qquad R_6 = Q_3^0 t_0 + \sum_{i=0}^{n-1} Q_8^{i+1} t_{i+1}$$

$$R_7 = A_{21}^0 \frac{t_0^2}{2} + \sum_{i=0}^{n-1} Q_8^{i+1} \left(\frac{h_{i+2}^2}{2} - \frac{h_{i+1}^2}{2} \right) \qquad R_8 = Q_4^0 t_0 + \sum_{i=0}^{n-1} Q_9^{i+1} t_{i+1}$$

$$R_9 = A_{22}^0 \frac{t_0^2}{2} + \sum_{i=0}^{n-1} Q_9^{i+1} \left(\frac{h_{i+2}^2}{2} - \frac{h_{i+1}^2}{2} \right) \qquad R_{10} = \sum_{i=0}^{n-1} Q_{10}^{i+1} t_{i+1}.$$

D. Reference strains in multilayer

The sum of total forces and moments can be equated to zero to satisfy the equilibrium conditions of the multilayer. As we have considered in the previous case, the sum of total bending force in the multilayer is zero, $\sum_{i=0}^{n} F_x^{B^i} = \sum_{i=0}^{n} F_y^{B^i} = 0$, which give rise to $\sum_{i=0}^{n} \left(F_x^{N^i} - F_x^{M^i} \right) = 0$ and $\sum_{i=0}^{n} \left(F_y^{N^i} - F_y^{M^i} \right) = 0$. We can evaluate the reference strains by using these conditions in terms of the strains arising from lattice and the thermal mismatch

$$\varepsilon_{xx}^N = \sum_{i=0}^{n} \left(\frac{\sigma_{xx}^{M^i} t_i}{Q_1^i t_i} \frac{\left[1 - \left(Q_2^i Q_3^i t_i / Q_1^i t_i \right) \right] t_i}{\left[Q_4^i - \left(Q_2^i Q_3^i t_i / Q_1^i t_i \right) \right] t_i} \right) - \sum_{i=0}^{n} \left(\frac{\sigma_{yy}^{M^i} t_i Q_2^i t_i}{Q_1^i t_i} \right)$$

$$\varepsilon_{yy}^N = \sum_{i=0}^{n} \left(\frac{\left[\sigma_{yy}^{M^i} - \sigma_{xx}^{M^i} \left(Q_3^i t_i / Q_1^i t_i \right) \right] t_i}{\left[Q_4^i - \left(Q_2^i Q_3^i t_i / Q_1^i t_i \right) \right] t_i} \right). \tag{10}$$

E. Reference curvatures and layer-wise electroelastic fields

The reference curvatures due to bending in the multilayer can be calculated by considering the moment equilibrium of the piezoelectric multilayer so that $\sum_{i=0}^{n} M_x^{Tot^i} = \sum_{i=0}^{n} \left(M_x^{N^i} + M_x^{B^i} - M_x^{M^i} \right) = 0$ and $\sum_{i=0}^{n} M_y^{Tot^i} = \sum_{i=0}^{n} \left(M_y^{N^i} + M_y^{B^i} - M_y^{M^i} \right) = 0$. These equations give the total curvature components as

$$K_x = \left[\frac{1}{S_1} + \frac{S_2 S_3}{S_1 \left(S_4 - S_2 S_3 / S_1 \right)} \right] \sum_{i=0}^{n} \left[M_x^{M^i} - M_x^{N^i} \right] - \frac{S_2}{\left(S_4 - S_2 S_3 / S_1 \right)} \sum_{i=0}^{n} \left[M_y^{M^i} - M_y^{N^i} \right]$$

$$K_y = \frac{1}{\left(S_4 - S_3 S_2 / S_1 \right)} \sum_{i=0}^{n} \left[\left(M_y^{M^i} - M_y^{N^i} \right) - \frac{S_3}{S_1} \left(M_x^{M^i} - M_x^{N^i} \right) \right], \tag{11}$$

where

$$S_1 = \left(\frac{A_{11}^0 t_0^3}{3} - \Pi_x Q_1^0 \frac{t_0^2}{2} \right) + \sum_{i=0}^{n-1} Q_5^{i+1} \left\{ \left(\frac{h_{i+2}^3}{3} - \frac{h_{i+1}^3}{3} \right) - \Pi_x \left(\frac{h_{i+2}^2}{2} - \frac{h_{i+1}^2}{2} \right) \right\}$$

$$S_2 = \left(A_{12}^0 \frac{t_0^3}{3} - \Pi_y Q_2^0 \frac{t_0^2}{2} \right) + \sum_{i=0}^{n-1} Q_6^{i+1} \left\{ \left(\frac{h_{i+2}^3}{3} - \frac{h_{i+1}^3}{3} \right) - \Pi_y \left(\frac{h_{i+2}^2}{2} - \frac{h_{i+1}^2}{2} \right) \right\}$$

$$S_3 = \left(A_{21}^0 \frac{t_0^3}{3} - \Pi_x Q_3^0 \frac{t_0^2}{2} \right) + \sum_{i=0}^{n-1} Q_8^{i+1} \left\{ \left(\frac{h_{i+2}^3}{3} - \frac{h_{i+1}^3}{3} \right) - \Pi_x \left(\frac{h_{i+2}^2}{2} - \frac{h_{i+1}^2}{2} \right) \right\}$$

$$S_4 = \left(A_{22}^0 \frac{t_0^3}{3} - \Pi_y Q_4^0 \frac{t_0^2}{2} \right) + \sum_{i=0}^{n-1} Q_9^{i+1} \left\{ \left(\frac{h_{i+2}^3}{3} - \frac{h_{i+1}^3}{3} \right) - \Pi_y \left(\frac{h_{i+2}^2}{2} - \frac{h_{i+1}^2}{2} \right) \right\}.$$

The total inplane normal stresses and the electric fields in each layer can be evaluated from the reference normal and bending strains, and the strains arising from the lattice and thermal mismatches. Superposing these components using Eqs. (5)–(8) yields,

$$\begin{aligned}\sigma_{xx}^{Tot^i} &= \sigma_{xx}^{N^i} + \sigma_{xx}^{B^i} - \sigma_{xx}^{M^i}\\ \sigma_{yy}^{Tot^i} &= \sigma_{yy}^{N^i} + \sigma_{yy}^{B^i} - \sigma_{yy}^{M^i}\\ E_{[0001]}^{Tot^i} &= E_{[0001]}^{N^i} + E_{[0001]}^{B^i} - E_{[0001]}^{M^i}.\end{aligned} \tag{12}$$

F. C-plane elastic multilayer

The c-plane in hexagonal crystals such as gallium nitride is the isotropic plane. Since this is the most popular growth orientation, it is worthwhile to deduce the results for the isotropic multilayer from the above general results. This can be done by substituting $\theta = \phi = 0$ in the rotation matrix. In this case, the orthogonal components of the inplane normal strain due to lattice misfit are the same, i.e., $\varepsilon_{xx}^m = \varepsilon_{yy}^m = \varepsilon^m$. Likewise, the curvatures due to bending in the multilayer become $K_x = K_y = K$, the positions of the neutral axes become $\Pi_x = \Pi_y = \Pi$, and the reference strains in the multilayer become $\varepsilon_{xx}^N = \varepsilon_{yy}^N = \varepsilon^N$. After introducing these simplifications, we can deduce the result for the isotropic elastic multilayer by letting the piezoelectric terms to vanish and converting the elastic constants to isotropic Young's Modulus, E, and Poisson's ratio, ν, as $C_{11} = E/(1-2\nu) = C_{33}$ and $C_{12} = C_{13} = E\nu/[(1+\nu)(1-2\nu)]$.

The position of the neutral axis for the elastic isotropic multilayer deduced from Eq. (9) can be expressed as

$$\Pi = \frac{1}{2}\sum_{i=0}^{n}\frac{E_i' t_i\,(h_{i+1}+h_i)}{E_i' t_i}, \tag{13}$$

where $E' = E/(1-\nu)$ is called biaxial Modulus. This can further be simplified by considering the substrate to be very thick in comparison to the film layers ($t_s \gg t_i$), thus, the position of the neutral axis can be expressed as

$$\Pi = \frac{t_0}{2}\left[1 + 2\sum_{i=1}^{n}\frac{E_i' t_i}{E_0' t_0}\right]. \tag{14}$$

With these assumptions, the reference strains given in Eq. (10) become

$$\varepsilon^N = \sum_{i=0}^{n}\frac{E_i' t_i\left(\varepsilon^{m^i} + \alpha_a^i \Delta T\right)}{E_i' t_i}, \tag{15}$$

which can be expressed as follows for the multilayer with very thick substrate

$$\varepsilon^N = \left[(\varepsilon^{m^0} + \alpha_a^0 \Delta T) + \sum_{i=1}^{n}\frac{E_i' t_i\left\{\varepsilon^{m^i} - (\alpha_a^0 - \alpha_a^i)\Delta T\right\}}{E_0' t_0}\right]. \tag{16}$$

Similarly, the curvature for the elastic multilayer can be obtained by simplifying Eq. (11)

$$K = \sum_{i=0}^{n}\frac{E_i'\left(\varepsilon^{m^i} + \alpha_a^i \Delta T - \varepsilon^N\right)\left(\frac{h_{i+1}^2}{2} - \frac{h_i^2}{2}\right)}{E_i'\left\{\left(\frac{h_{i+1}^3}{3} - \frac{h_i^3}{3}\right) - \Pi\left(\frac{h_{i+1}^2}{2} - \frac{h_i^2}{2}\right)\right\}}. \tag{17}$$

This can further be simplified for the case of thick substrate

$$K = 3\sum_{i=0}^{n}\frac{E_i' t_i\left\{\varepsilon^{m^i} - (\alpha_a^0 - \alpha_a^i)\Delta T\right\}}{E_0' t_0^2}. \tag{18}$$

These results provided in Eqs. (13), (15) and (17) are identical to the ones given by Gao et al.[10] in the absence of lattice misfit strain, ε^m.

III. GALLIUM NITRIDE MULTI QUANTUM WELL DEVICE

To illustrate the applicability of the present analytical model, the specific results for a gallium nitride-based multi quantum well device consisting of 12 film layers deposited on a sapphire substrate for *c*-, *a*- and *m*-growth orientations have been considered. A schematic representation of the quantum well layers in a LED device with it's thickness and material constituents are shown in Fig. 2. The material properties of Sapphire (Al_2O_3), gallium nitride (GaN), indium nitride (InN) and aluminum nitride (AlN) are provided in Appendix B. The Vegard's law was used to calculate the material properties of alloyed layers.[24] The deposition temperature was considered to be 1000^0C. The inplane strains due to lattice misfit between the consecutive film layers are also provided in Appendix B. The misfit strains between the substrate and the buffer layer are very high, which can induce a large number of defects such as misfit dislocation in actual devices. Although the strains of this magnitude are outside the validity of linear piezoelectricity, we nevertheless used them to evaluate the stresses and the electric fields in each quantum well layer. To be formal, one would have to invoke a theory of misfit dislocation density predictions to properly relieve the excessive strains that are built up in the strained layers.

In order to confirm the results of our analytical model, GaN-based piezoelectric multilayer was modeled using the commercial finite element analysis code ABAQUS 6.14. The FEM results for various growth orientations have been obtained by utilizing the 3-D piezoelectric elements and appropriately changing the material properties.

The inplane stress distributions evaluated analytically and by the finite element analysis in each layer of the multi quantum well for *c*-plane growth orientation have been plotted in Fig. 3. The results were obtained for both piezoelectric and elastic multilayers. An excellent agreement between the results evaluated using the closed-form expressions and the FEM analysis was observed. It is observed that the presence of piezoelectricity increases the stress marginally. Even though the bending stresses vary linearly with z in each layer, the inplane components are shown to be constant throughout the thickness indicating that the misfit normal strains dominate in each layer. It has also been found that the contribution of lattice misfit on the total reference strain components are almost twice that of the thermal mismatch, albeit with opposite sign for all growth orientations. Layer-wise stresses are discontinuous at the interfaces as the mismatch strains and the material properties of each layers are different (Table I, Appendix B).

Figure 4 and 5 show inplane stress distributions in the elastic and piezoelectric multi quantum well for *a*- and *m*-plane growth orientations, respectively. In these cases also, both the analytical and FEM results were obtained. It is interesting to note that for the *m*-plane growth, the bending along $[11\bar{2}0]$ crystal direction occurs in the opposite direction from the other orientation. This

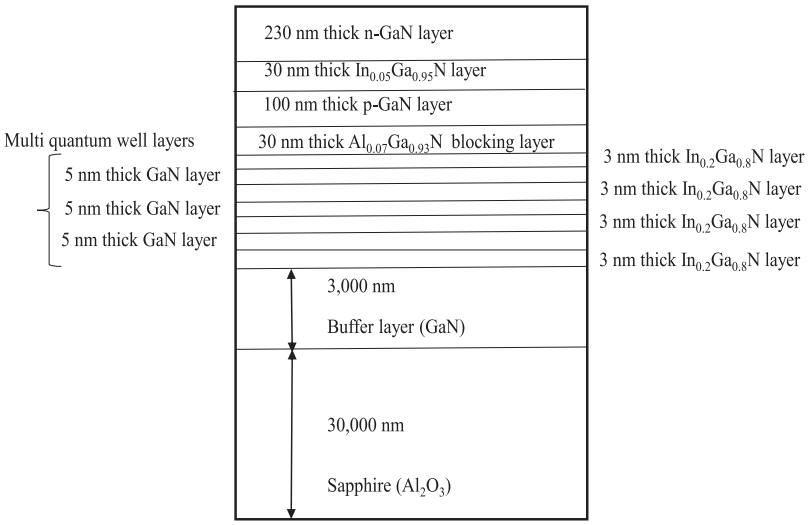

FIG. 2. Schematic representation of different layers in LED device.

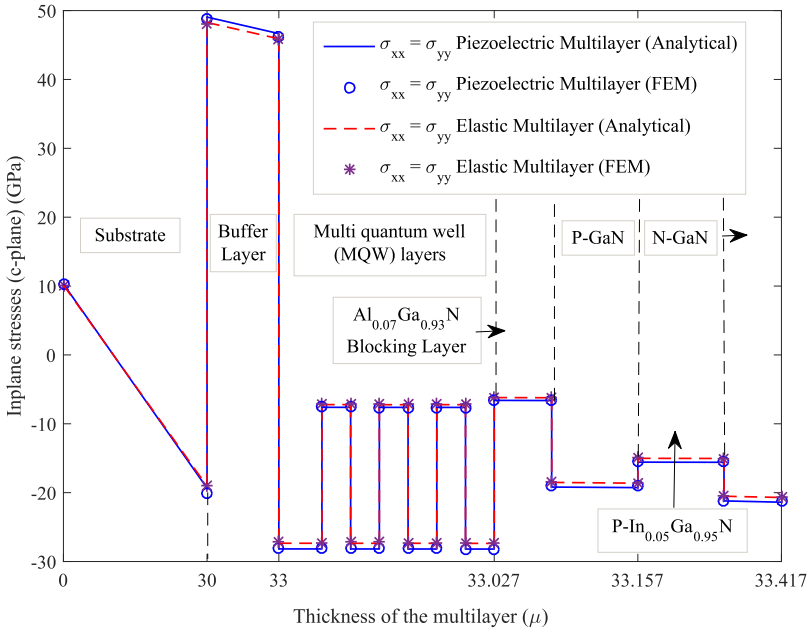

FIG. 3. Inplane stresses in elastic and piezoelectric *c*-plane multi quantum well (MQW).

is because of the very high extensional lattice misfit strain in this particular orientation which is opposite to other growth orientations considered in this work. In the *a*-plane growth, the stress component, σ_{xx}, along $[1\bar{1}00]$ crystal direction increases due to piezoelectricity in the multi quantum well layers. The inplane stress component, σ_{yy}, along [0001] crystal direction increases due to piezoelectricity in *InGaN* layers while it decreases in *GaN* layers for the *a*-plane growth (Fig. 4). In the *m*-plane growth, both σ_{xx} and σ_{yy} along [0001] and $[11\bar{2}0]$ crystal directions, respectively, increase in the *GaN* layers while they decrease in the *InGaN* layers (Fig. 5). Although, the effects of piezoelectricity on strains are very small in all growth orientations, nevertheless,

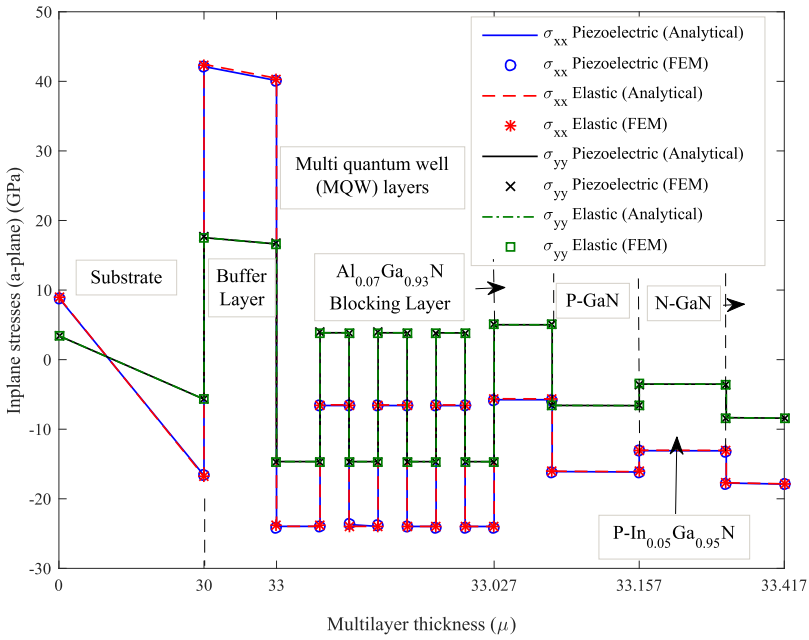

FIG. 4. Inplane stresses in elastic and piezoelectric *a*-plane multi quantum well (MQW).

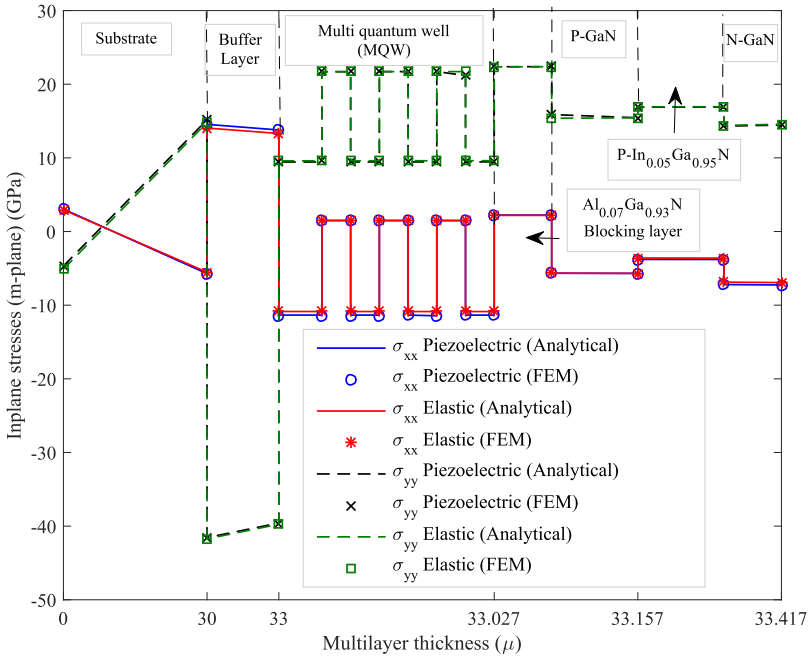

FIG. 5. Inplane stresses in elastic and piezoelectric *m*-plane multi quantum well (MQW).

accurate predictions of piezoelectrically generated electric fields are important in correctly predicting the optoelectronic performance of the device. The electric field along the growth direction combined with the spontaneous polarization can cause weaker recombination probability[25] which contributes to the band bending that reduces the quantum efficiency and lowers the performance of the device.[26–28] Therefore, it is important to consider the effects of piezoelectricity in the analysis.

The distribution of electric field along [0001] direction obtained both analytically and by finite element analysis has been shown in Fig. 6 for all three growth orientations. It is observed that the magnitude of the electric field in the *c*- and *a*-plane growth orientation is very high (1.4 GV/m) in

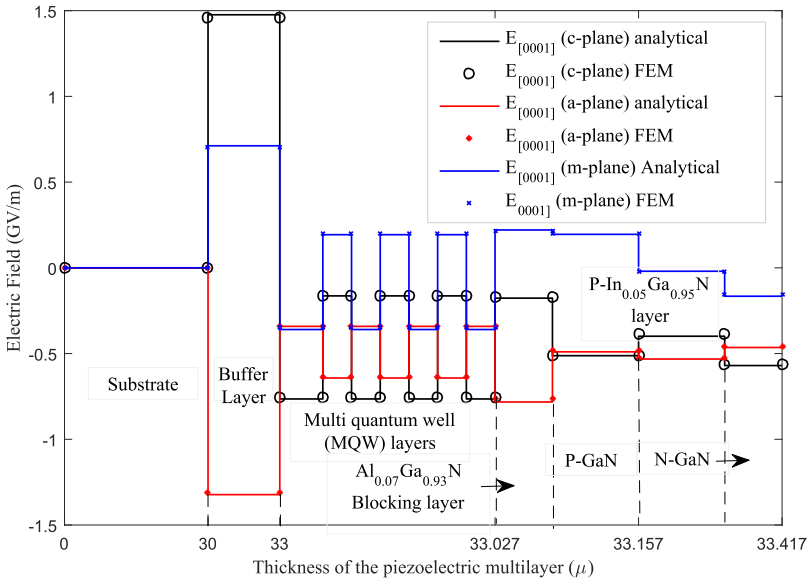

FIG. 6. Distribution of electric field along [0001] crystal direction in various growth orientations.

comparison to the the electric fields in the *m*-plane growth. However, the high electric field induced in the buffer layer gets reduced by an order magnitude in the multi quantum well region (e.g., 746 MV/m in $In_{0.2}Ga_{0.8}N$ layers and 160 MV/m in GaN layers). As expected, the electric field in the *c*-plane is along the growth direction while in other two planes it is perpendicular to the growth directions.

IV. CONCLUSION

We derived the closed-form expressions for the electroelastic fields in piezoelectric hexagonal multilayers with lattice and thermal mismatch between the reference substrate and the deposited film layers. The solution can model any number of layers. The closed-form expressions derived herein is capable of evaluating the electroelastic fields in each layer having various growth orientations. The results for the purely elastic isotropic multilayer were deduced by letting the elastic constants to be isotropic and the piezoelectric terms to vanish. These results agree with those given by Gao et al. for elastic multilayers[10] which can further be simplified to match the text book results based on the Stoney formula. To validate the analytical results, multi quantum well layers with *c*-, *a*- and *m*-growth orientations were also modeled by the commercial finite element analysis code ABAQUS 6.14. An excellent agreement between the analytical and FEM results was observed for both inplane stresses and electric fields. The effects of piezoelectricity on inplane stresses and electric fields in a piezoelectric multi quantum well device have also been discussed. The high lattice mismatch turns out to be the major contributor for inplane reference and bending strains in the piezoelectric multilayer. The closed-form expressions derived herein can be a useful tool in quickly predicting the state of electroelastic fields in piezoelectric multilayers consisting of hexagonal crystals. These results will also be helpful in predicting the optoelectronic performance of multi quantum wells with correctly predicted strains and piezoelectrically induced electric fields.

SUPPLEMENTARY MATERIAL

See supplementary material for Matlab figure files for stresses and electric field variations with multilayer thickness have been provided as supplementary material.

ACKNOWLEDGMENTS

This work was supported by the Korea National Research Foundation with the grants NRF-2014M1A3A3A02034928 and NRF-2016R1D1A1B03932553.

APPENDIX A

Constitutive relations for piezoelectric materials with *z*-direction as c-axis exhibiting transversely isotropic behavior (hexagonal symmetry) can be written in the form[29]

$$\begin{Bmatrix}\sigma_{xx}\\ \sigma_{yy}\\ \sigma_{zz}\\ \sigma_{zy}\\ \sigma_{zx}\\ \sigma_{xy}\end{Bmatrix} = \begin{bmatrix} c_{11} & c_{12} & c_{13} & 0 & 0 & 0 \\ c_{12} & c_{11} & c_{13} & 0 & 0 & 0 \\ c_{13} & c_{13} & c_{33} & 0 & 0 & 0 \\ 0 & 0 & 0 & c_{44} & 0 & 0 \\ 0 & 0 & 0 & 0 & c_{44} & 0 \\ 0 & 0 & 0 & 0 & 0 & \frac{1}{2}(c_{11}-c_{12}) \end{bmatrix} \begin{Bmatrix}\varepsilon_{xx}\\ \varepsilon_{yy}\\ \varepsilon_{zz}\\ 2\varepsilon_{zy}\\ 2\varepsilon_{zx}\\ 2\varepsilon_{xy}\end{Bmatrix} - \begin{bmatrix} 0 & 0 & e_{31} \\ 0 & 0 & e_{31} \\ 0 & 0 & e_{33} \\ 0 & e_{15} & 0 \\ e_{15} & 0 & 0 \\ 0 & 0 & 0 \end{bmatrix} \begin{Bmatrix}E_x\\ E_y\\ E_z\end{Bmatrix}$$

$$\begin{Bmatrix}D_x\\ D_y\\ D_z\end{Bmatrix} = \begin{bmatrix} 0 & 0 & 0 & 0 & e_{15} & 0 \\ 0 & 0 & 0 & e_{15} & 0 & 0 \\ e_{31} & e_{31} & e_{33} & 0 & 0 & 0 \end{bmatrix} \begin{Bmatrix}\varepsilon_{xx}\\ \varepsilon_{yy}\\ \varepsilon_{zz}\\ 2\varepsilon_{zy}\\ 2\varepsilon_{zx}\\ 2\varepsilon_{xy}\end{Bmatrix} - \begin{bmatrix} \epsilon_{11} & 0 & 0 \\ 0 & \epsilon_{11} & 0 \\ 0 & 0 & \epsilon_{33} \end{bmatrix} \begin{Bmatrix}E_x\\ E_y\\ E_z\end{Bmatrix} + \begin{Bmatrix}0\\ 0\\ P_{sp}\end{Bmatrix}. \tag{A1}$$

APPENDIX B

The misfit strains[30] in different layers can be expressed in Table I as

TABLE I. Misfit strains due to lattice mismatch between the substrate and different film layers for various growth orientations.

	c-plane growth	*a*-plane growth	*m*-plane growth
Substrate and	ε_{xx}^{m} = -0.133	ε_{xx}^{m} = -0.16	ε_{xx}^{m} = -0.022
GaN layers	ε_{yy}^{m} = -0.133	ε_{yy}^{m} = -0.03	ε_{yy}^{m} = 0.162
GaN and	ε_{xx}^{m} = 0.022	ε_{xx}^{m} = 0.022	ε_{xx}^{m} = 0.022
$In_{0.2}Ga_{0.8}N$ layers	ε_{yy}^{m} = 0.022	ε_{yy}^{m} = 0.022	ε_{yy}^{m} = 0.022
$In_{0.2}Ga_{0.8}N$ and	ε_{xx}^{m} = -0.022	ε_{xx}^{m} = -0.022	ε_{xx}^{m} = -0.022
GaN layers	ε_{yyy}^{m} = -0.022	ε_{yy}^{m} = -0.022	ε_{m_y} = -0.022
$In_{0.2}Ga_{0.8}N$ and	ε_{xx}^{m} = -0.02428	ε_{xx}^{m} = -0.02428	ε_{xx}^{m} = -0.02428
$Al_{0.07}Ga_{0.93}N$ layers	ε_{yy}^{m} = -0.02428	ε_{yy}^{m} = -0.02428	ε_{yy}^{m} = -0.02428
$Al_{0.07}Ga_{0.93N}$ and	ε_{xx}^{m} = 0.0016	ε_{xx}^{m} = 0.0016	ε_{xx}^{m} = 0.0016
GaN layers	ε_{yy}^{m} = 0.0016	ε_{yy}^{m} = 0.0016	ε_{xx}^{m} = 0.0016
GaN and	ε_{xx}^{m} = -0.0055	ε_{xx}^{m} = -0.0055	ε_{xx}^{m} = -0.0055
$In_{0.05}Ga_{0.95}N$ layer	ε_{yy}^{m} = -0.0055	ε_{yy}^{m} = -0.0055	ε_{yy}^{m} = -0.0055
$In_{0.05}Ga_{0.95}N$ and	ε_{xx}^{m} = 0.0055	ε_{xx}^{m} = 0.0055	ε_{xx}^{m} = 0.0055
GaN layer	ε_{yy}^{m} = 0.0055	ε_{yy}^{m} = 0.0055	ε_{yy}^{m} = 0.0055

The material properties of the substrate (Al_2O_3),[31] gallium nitride (GaN),[32,33] Aluminum nitride (AlN)[33] and Indium nitride (InN)[34] are listed in Table II as

TABLE II. Material properties.

Material	Elastic constants (GPa)	Piezoelectric constants (C/m^2)	Dielectric constants $\times 10^{-12}$ (C/Vm)	Coefficient of Thermal expansion $(10^{-6})\ /^0C$
	c_{11} = 497.6			α_a = 5.22
Sapphire	c_{12} = 162.6	e_{31} = 0	ϵ_{33} = 11.54	α_c = 7.77
(Al_2O_3)	c_{13} = 115.5	e_{33} = 0		
	c_{33} = 503.3		Spontaneous polarization,	
	c_{44} = 147.4		P_{sp} = 0 C/m^2	
	c_{11} = 367			α_a = 4.15
Gallium	c_{12} = 135	e_{31} = -0.49	ϵ_{33} = 92.925	α_c = 5.27
Nitride	c_{13} = 103	e_{33} = 0.73		
(GaN)	c_{33} = 405		Spontaneous polarization,	
	c_{44} = 95		P_{sp} = –0.029 C/m^2	
	c_{11} = 223			α_a = 2.7
Indium	c_{12} = 115	e_{31} = -0.49	ϵ_{33} = 99.93	α_c = 3.4
Nitride	c_{13} = 92	e_{33} = 0.73		
(InN)	c_{33} = 224		Spontaneous polarization,	
	c_{44} = 48		P_{sp} = –0.032 C/m^2	
	c_{11} = 396			α_a = 4.2
Aluminum	c_{12} = 137	e_{31} = -0.58	ϵ_{33} = 94.67	α_c = 5.3
Nitride	c_{13} = 108	e_{33} = 1.55		
(AlN)	c_{33} = 373		Spontaneous polarization,	
	c_{44} = 116		P_{sp} = –0.081 C/m^2	

[1] G. G. Stoney, Proc. R. Soc. Lond. A **82**, 172–175 (1909).
[2] P. H. Townsend and D. M. Barnett, J. App. Phys. **62**(11), 4438–4444 (1987).
[3] L. B. Freund, J. Mech. Phys. Sols. **44**(5), 723–736 (1996).
[4] L. B. Freund, J. Crys. Grwth. **132**, 341–344 (1993).
[5] N. H. Zhang, Thi. Sol. Films **515**, 8402–8406 (2007).
[6] Y. Y. Hu and W. M. Huang, J. Appl. Phys. **96**, 4154–4160 (2004).
[7] X. Feng, Y. Huwang, and A. J. Rosakis, Int. J. Sol. Structs. **45**, 3688–3698 (2008).

[8] X. Feng, Y. Huwang, and A. J. Rosakis, J. Appl. Mech. **75**, 021022-1–021022-7 (2008).
[9] C. H. Hsueh, L. C. De Jonghe, and C. S. Lee, J. Am. Soc. **89**(1), 251–257 (2006).
[10] C. Gao, Z. Zhao, and X. Li, J. App. Phys. **117**, 055305 (2015).
[11] R. Ali, D. R. Mahapatra, and S. Gopalakrishnan, Sensors and Actuators **116**, 424–437 (2004).
[12] X. F. Li and K. Y. Lee, Smat Mater. Struct. **13**, 424–432 (2004).
[13] F. Narita, Y. Shindo, and K. Hayashi, Comp. and Struct. **83**, 1164–1170 (2005).
[14] M. Dems and W. Nakwaski, Semicond. Sci. Technol. **18**, 733–737 (2003).
[15] C. M. A. Vasques and J. D. Rodrigues, Int. J. Num. Methds. in Engg. **62**, 1488–1518 (2005).
[16] H.-Y. Zhang and B. L. Wang, J. Therm. Sci. **31**, 246–259 (2008).
[17] S. Vitroz, L. Rufer, G. Rehder, U. Heinel, and P. Benkart, Sensrs. Actrs. A: Physic. **172**, 27–34 (2011).
[18] F. Narita, T. Sasakura, and F. Narita, J. Eng. Mat. Tech. **134**, 031007-1–031007-7 (2012).
[19] F. Narita, R. Hasegawa, and Y. Shindo, J. Appl. Phys. **115**, 184103 (2014).
[20] S. Yuan, Y. Zhao, X. Chu, C. Zhu, and Z. Zhong, Appl. Sci. **225**(6), 1–12 (2016).
[21] M. N. G. Nejhad, C. Pan, and H. Feng, J. Elect. Packaging **125**, 4–17 (2003).
[22] D. H. Jang, K. Yoo, J. I. Shim, and J. Kor, Phys. Soc. **57**(4), 787–792 (2010).
[23] U. M. E. Christmas, A. D. Andreev, and D. A. Faux, J. Appl. Phys. **98**, 073522 (2005).
[24] A. R. Denton and N. W. Ashcroft, Physical Review A **43**(6), 3161–3164 (1991).
[25] D. A. B. Miller, D. S. Chemla, T. C. Damen, A. C. Gossard, W. Wiegmann, T. H. Wood, and C. A. Burrs, Phys. Rev. Lett. **53**(22), 2173–2176 (1984).
[26] R. A. Beach and T. C. McGill, J. Vac. Sci. Tech., B **17**(4), 1753–1756 (1999).
[27] C. Wetzel, T. Takeuchi, H. Amano, and I. Akasaki, III-Nitride Semiconductors: Optical Properties II (Taylor and Francis, Newyork, 2002), pp. 219–258.
[28] I. K. Park, M.-K. Kwon, C.-Y. Cho, J.-Y. Kim, C.-H. Cho, and S.-J. Park, Appl. Phys. Lett. **92**(1-3), 253105 (2008).
[29] D. A. Berlincourt, D. R. Curran, and H. Jaffe, Phycl. Acoust. 1A (ed.) W. P. Mason, Academic Press, New York, 177 (1964).
[30] Q. Sun and J. Han, GaN and ZnO based Materials and Devices 156, Springer Series in Material Science (Heidelberg, Berlin, 2012).
[31] A. Palino, M. Grimsditch, and I. Grzegory, J. Appl. Phys. **79**(6), 3343–3344 (1996).
[32] V. Bougrov, M. E. Levinshtein, S. L. Rumyantsev, and A. Zubrilov, Properties of Advanced Semiconductor Materials . John Wiley & Sons, Inc., New York, 1-30 (2001).
[33] T. Vodenitcharova, L. C. Zhang, I. Zarudi, Y. Yin, H. Domyoc, T. Hoc, and M. Sato, J. of Mat. Proces. Tech. **194**, 52–62 (2007).
[34] K. Kim, W. R. L. Lambrecht, and B. Segall, Phy. Rev. B **53**(24), 16310–16326 (1996).